Modules in the brain stem and spinal cord underlying motor behaviors

Jinsook Roh, Vincent C. K. Cheung and Emilio Bizzi

You might find this additional info useful...

This article cites 68 articles, 42 of which can be accessed free at:
http://jn.physiology.org/content/106/3/1363.full.html#ref-list-1

Updated information and services including high resolution figures, can be found at:
http://jn.physiology.org/content/106/3/1363.full.html

Additional material and information about *Journal of Neurophysiology* can be found at:
http://www.the-aps.org/publications/jn

This infomation is current as of September 8, 2011.

Modules in the brain stem and spinal cord underlying motor behaviors

Jinsook Roh,[1,2] **Vincent C. K. Cheung,**[1] **and Emilio Bizzi**[1]

[1]*McGovern Institute for Brain Research and Department of Brain and Cognitive Sciences, Massachusetts Institute of Technology, Cambridge, Massachusetts; and* [2]*Sensory Motor Performance Program, Rehabilitation Institute of Chicago, and Department of Physical Medicine and Rehabilitation, Feinberg School of Medicine, Northwestern University, Chicago, Illinois*

Roh J, Cheung VC, Bizzi E. Modules in the brain stem and spinal cord underlying motor behaviors. *J Neurophysiol* 106: 1363–1378, 2011. First published June 8, 2011; doi:10.1152/jn.00842.2010.— Previous studies using intact and spinalized animals have suggested that coordinated movements can be generated by appropriate combinations of muscle synergies controlled by the central nervous system (CNS). However, which CNS regions are responsible for expressing muscle synergies remains an open question. We address whether the brain stem and spinal cord are involved in expressing muscle synergies used for executing a range of natural movements. We analyzed the electromyographic (EMG) data recorded from frog leg muscles before and after transection at different levels of the neuraxis—rostral midbrain (brain stem preparations), rostral medulla (medullary preparations), and the spinal-medullary junction (spinal preparations). Brain stem frogs could jump, swim, kick, and step, while medullary frogs could perform only a partial repertoire of movements. In spinal frogs, cutaneous reflexes could be elicited. Systematic EMG analysis found two different synergy types: *1*) synergies shared between pre- and posttransection states and *2*) synergies specific to individual states. Almost all synergies found in natural movements persisted after transection at rostral midbrain or medulla but not at the spinal-medullary junction for swim and step. Some pretransection- and posttransection-specific synergies for a certain behavior appeared as shared synergies for other motor behaviors of the same animal. These results suggest that the medulla and spinal cord are sufficient for the expression of most muscle synergies in frog behaviors. Overall, this study provides further evidence supporting the idea that motor behaviors may be constructed by muscle synergies organized within the brain stem and spinal cord and activated by descending commands from supraspinal areas.

motor control; motor primitives; electromyography; non-negative matrix factorization

THE CENTRAL NERVOUS SYSTEM (CNS) and the musculoskeletal system of animals cooperate to generate purposeful, well-coordinated behaviors. Previous studies have suggested that the CNS simplifies the control of many degrees of freedom of the musculoskeletal system by activating a small number of movement modules (Bizzi et al. 1991, 2008; Fetz et al. 2000; Grillner 1985; Miller 2004; Tresch et al. 1999, 2002). Experimental evidence accumulated to date has supported the idea that movement modules could be operationally defined as muscle synergies, characteristic patterns of simultaneous muscle activations, whose combination could produce a variety of movements (Hart and Giszter 2004; Ting and Macpherson 2005; Tresch et al. 1999, 2002). Some studies have exploited this framework of muscle synergy to understand natural movements found in intact animals and humans, including terrestrial and aquatic movements in the frog (d'Avella et al. 2003; d'Avella and Bizzi 2005), postural responses in the cat (Lockhart and Ting 2007; McKay and Ting 2008; Ting and Macpherson 2005; Torres-Oviedo et al. 2006), locomotion in the cat (Krouchev et al. 2006), whole arm reaching in the cat (Yakovenko et al. 2011), grasping and reaching in the monkey (Overduin et al. 2008), as well as postural responses (Krishnamoorthy et al. 2003; Torres-Oviedo and Ting 2007, 2010; Weiss and Flanders 2004), locomotion (Cappellini et al. 2006; Clark et al. 2010; Ivanenko et al. 2007; Monaco et al. 2010), and arm movements (d'Avella et al. 2006; Muceli et al. 2010; Sabatini 2002) in humans. Others have investigated behaviors in reduced preparations, often spinalized animals, to address the issue of modularity in the organization of neural circuitries (Giszter and Kargo 2000; Kargo and Giszter 2000a, 2000b; Saltiel et al. 1998, 2001, 2005; Stein et al. 1995; Tresch et al. 1999).

Despite the wealth of previous studies on muscle synergies in spinalized and intact animal preparations, where in the CNS muscle synergies are organized remains an unanswered question. Muscle synergies responsible for natural behaviors could entirely be organized within the spinal cord. Stein and his colleagues have obtained evidence from the spinalized turtle, showing that motor patterns during scratching are generated by a central pattern generator in the spinal cord comprising ipsilateral and contralateral modules for flexors and extensors (Mortin et al. 1985; Robertson et al. 1985; Stein et al. 1995). In the mud puppy, separate burst generators in the spinal cord for forelimb flexion and extension during walking have been identified as well (Cheng et al. 1998). In the frog, repetitive microstimulation in the lumbar spinal cord evoked only a few stereotypical ankle force patterns representable as force fields (Bizzi et al. 1991; Giszter and Kargo 2000). Focal intraspinal NMDA iontophoresis applied to interneurons in the frog spinal cord (Saltiel et al. 1998, 2001, 2005) demonstrated the existence of spinal modules organized as patchy structures in the lumbar region. Studies of spinal wiping reflexes in the frog also show that the frog wiping motor patterns can be constructed as a time-varying summation of the force field primitives found with spinal stimulation (Giszter et al. 1993; Kargo and Giszter 2000a, 2000b). Using single-cell recordings and information theory-guided analyses, another recent study also supports the idea that activities of individual interneurons in the spinal cord are involved in expressing muscle synergies (Hart and Giszter 2010). The experiments summarized above, all performed on spinalized amphibians and reptiles, argue that motor patterns produced by the spinal cord alone are decomposable into numerous movement modules, implying that some of the

Address for reprint requests and other correspondence: J. Roh, Sensory Motor Performance Program, Rehabilitation Inst. of Chicago, Physical Medicine and Rehabilitation, Feinberg School of Medicine, Northwestern Univ., Rm. 1406, 360 E Superior St., Chicago, IL 60611 (e-mail: j-roh@northwestern.edu).

muscle synergies used for natural behaviors are likely organized within the spinal interneuronal networks.

Beside the spinal cord, the brain stem nuclei may also be responsible for structuring muscle synergies used for natural behaviors. This is underscored by previous physiological and anatomic studies showing that in the frog reticulospinal and vestibulospinal fibers establish direct monosynaptic connections with lumbar motoneurons (Barale et al. 1971; Cruce 1974; Magherini et al. 1974; Shapovalov 1975). The wide distribution of these downstream fibers suggests that they may be well suited for producing the extensor and flexor movements characteristic of frog locomotion. In addition, descending connections from the contralateral optic tectum to the ventral horn of the cervical spinal cord have also been found in the leopard frog (Rubinson 1968). The above anatomic studies suggest that both the midbrain and hindbrain, in addition to the spinal cord, may potentially structure some of the synergies used for constructing natural motor behaviors.

The studies reviewed above all point to the picture that the brain stem and/or spinal cord organize discrete muscle synergies. Here we sought to investigate whether the muscle synergies used by an intact animal for constructing natural motor behaviors are organized by brain stem and/or spinal cord neurons. Specifically, we recorded EMGs from all major hindlimb muscles of the frog during a variety of natural movements before and after the neuraxis was severed at three different levels, disconnecting structures above the midbrain, medulla, and spinal cord, respectively, from the motoneuronal pools. These transection experiments have allowed us to identify the minimal set of CNS structures necessary for the expression of muscle synergies used during natural behaviors, aiding us also to localize where in the CNS these synergies are expressed.

MATERIALS AND METHODS

Surgeries

All procedures were approved by the Committee on Animal Care at the Massachusetts Institute of Technology (MIT) before experimentations. Nine adult bullfrogs (*Rana catesbeiana*, 218–396 g) were studied: three for comparing behaviors before and after transection at the rostral end of the midbrain (a brain stem preparation; Fig. 1*B*), three for the rostral end of the medulla (a medullary preparation; Fig. 1*C*), and three for the rostral end of the spinal cord (a spinal preparation; Fig. 1*D*). Two surgeries were performed on each frog on separate days: one for implantation of EMG electrodes and the other for transection of the CNS. After injection of 0.1 mg/g tricaine (MS-222, Sigma) into the dorsal lymph sac for anesthesia, the frog was kept on a pad of crushed ice over the entire surgery to prolong the anesthetic effect of tricaine.

During the first surgery, in order to implant bipolar EMG electrodes into the muscles the skin was incised on the dorsal and ventral surfaces of the thigh and on the dorsal surface of the calf. The implanted hindlimb muscles were rectus internus (RI), adductor magnus (AD), semitendinosus (ST), sartorius (SA), vastus internus (VI), rectus anterior (RA), vastus externus (VE), iliopsoas (IP), biceps femoris (BI), semimembranosus (SM), gastrocnemius (GA), tibialis anterior (TA), and peroneus (PE) (nomenclature of Ecker 1971). Most of these muscles are biarticular. RI, ST, and SM are both hip extensors and knee flexors, while AD is a hip extensor; VE, VI, and RA are both hip flexors and knee extensors; BI and SA are both hip flexors and knee flexors, while IP is a hip flexor; GA is both a knee flexor and an ankle extensor, while PE and TA are both knee extensors and ankle flexors. The signs of the moment arms of these muscles are based on the results of Cajigas-González (2003) and Kargo and Rome (2002). This set of muscles includes all major muscles of the frog hindlimb. Each pair of electrodes used consisted of two multistrained Teflon-coated stainless steel wires (A-M Systems, Calsborg, WA) knotted together. On each, 1–2 mm of wires was stripped off the Teflon coat for signal pickup. After the electrodes were implanted into the
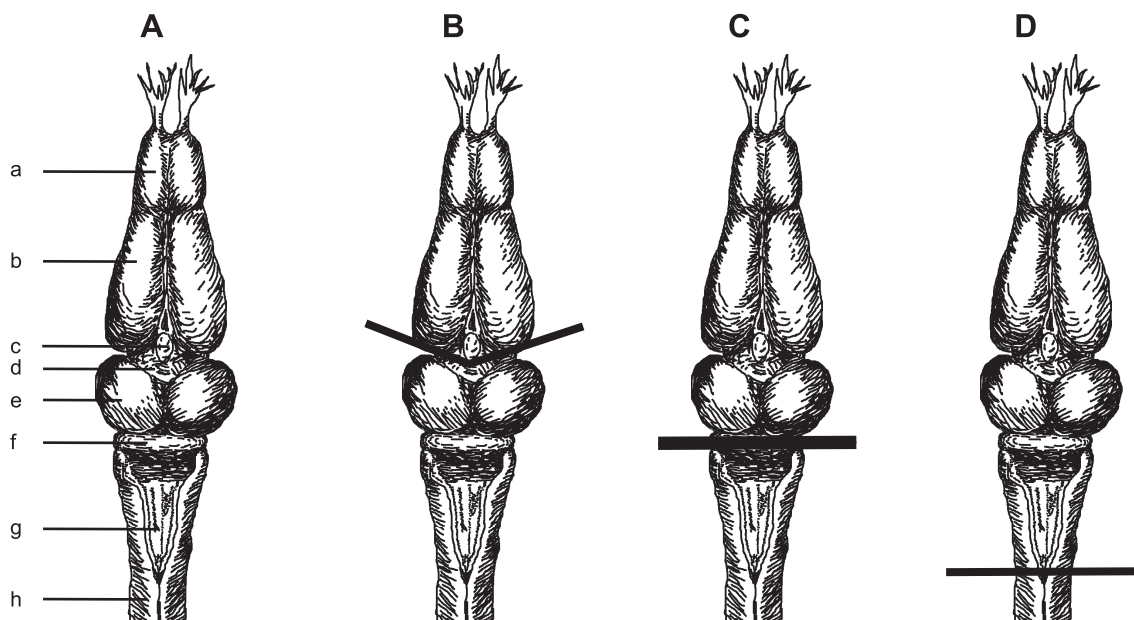

Fig. 1. Schematic diagram of the bullfrog central nervous system (CNS) and transection at 3 different levels of the neuraxis. *A*: the bullfrog CNS. a, Olfactory lobes; b, cerebral hemispheres; c, pineal gland; d, thalamus; e, optic lobes; f, cerebellum; g, medulla; h, spinal cord. *B*: in the 1st set of experiments (intact vs. brain stem conditions), transection was performed at the level (marked by a solid line) of the caudal end of the 3rd ventricle to keep the entire brain stem connected to the musculoskeletal system. *C*: in the 2nd set of experiments (intact vs. medullary conditions), the level of transection was at the caudal end of the pons (by removing the deep cerebellar nuclei). *D*: in the 3rd set of experiments (intact vs. spinal conditions), spinalization was performed at the level of caudal end of the 4th ventricle. In this preparation, there was no descending command going to the spinal cord. For each set of comparisons, EMG data were recorded both before and after transection in the same animal.

muscles with surgical needles, the wires were guided subcutaneously to the frog's back. All 13 pairs of electrodes were connected to a 37-pin miniature d-sub connector secured to the back skin with a custom-made plastic platform and Nexaband glue (Veterinary Products Laboratories, Phoenix, AZ). Crimp contacts were insulated by both epoxy and dental wax.

During the second surgery, the CNS of the same animal was transected at various levels of the neuraxis. After the cervico-medullary junction was exposed, the frog's CNS was severed, with fine scissors and forceps, at the level of the caudal end of the third ventricle for the brain stem preparation, at the caudal end of the pons (thus also removing the deep cerebellar nuclei) for the medullary preparation, or at the caudal end of the fourth ventricle for the spinal preparation. Complete separation was ensured by small pieces of gelfoam inserted into the cut. Between surgeries and experimental sessions, the frog was allowed at least 1 day for recovery. Transected frogs were kept in a refrigerator at 9°C between surgeries and experiments.

Experimental Procedures

Three different experiments were performed: comparison of EMGs and behaviors between the intact versus brain stem conditions, between the intact versus medullary conditions, and between the intact versus spinal conditions. Each experiment involved implantation of EMG electrodes, recording natural motor behaviors of the intact frog, CNS transection, and, finally, recording behaviors of the reduced preparation. The motor behaviors of the different preparations we observed included jump, swim, kick, and step and cutaneous reflexes of the spinal preparation. A few episodes of jumping, swimming, kicking, and stepping were spontaneous, but most of them were elicited by lightly scratching or pinching the skin with a pair of sharp forceps at sites ipsilateral or contralateral to the recorded hindlimb, including the rostral and dorsal surfaces of the hindlimb, the web of the foot, the toes, the caudal surface of the thigh, and the region around the cloacal fold. These sites of cutaneous stimulation were selected because their stimulations consistently yielded EMG signals with minimal artifacts. Episodes of both in-phase and out-of-phase swimming were either spontaneous or elicited by mildly touching the hindlimbs with a plastic rod. During all swimming trials, removable light-bodied Permlastic (Kerr USA, Romulus, MI) was used for waterproofing of the EMG-electrode connector. All behavioral trials were videotaped, and EMGs were recorded during all behavioral types. Video and EMG recordings were synchronized by a digital counter. After all experimental procedures, correct placement of electrodes in muscles was confirmed in postmortem dissections.

Data Collection and Preprocessing

All recorded EMGs were band-pass filtered (10 Hz to 1 kHz), amplified (gain of 10,000), and digitized at 1 kHz through differential current amplifiers. With custom software written in Matlab (MathWorks, Natick, MA), the continuous EMG signals were manually parsed into segments, each containing a single episode of jumping, kicking, stepping cycles, swimming cycles, or spinal reflexes. The parsed EMG data were subsequently high-pass filtered (window-based finite impulse response filter with cutoff frequency of 50 Hz and order 50) to remove any movement artifacts. The data were then rectified, low-pass filtered (cutoff frequency of 20 Hz and order 50) to remove noise, and integrated over 10-ms intervals.

Data Analysis

When designing our experimental procedure, we sought to study the functional differences between the different neural divisions in the CNS, under the framework of muscle synergies, by varying the level of transection at three different levels. We hypothesize that the synergies found in an animal after transection are similar to the synergies underlying movements in the same animal's intact state, thus implying that the neural divisions left connected to the musculoskeletal system play a role in specifying and activating the observed synergies. Our analysis therefore consisted of *1*) extracting muscle synergies underlying movements in different conditions and *2*) comparing the synergies observed before and after transection in the same animal.

Synergy Extraction

Separate extraction of synergies to assess EMG dimensionalities. We modeled EMG patterns as linear combination of a set of time-invariant synergies, each of which represents the balance of muscle activation across 12 or 13 muscles (Cheung et al. 2005, 2009; Hart and Giszter 2004; Torres-Oviedo et al. 2006; Tresch et al. 1999, 2006). Excepting muscles BI in *animal m1* and IP in *animal s2*, which were not recorded, EMG responses from all 13 muscles were recorded in all animals across all behavioral conditions (Table 1). The nonnegative matrix factorization algorithm (NMF; Lee and Seung 1999, 2001) was applied to the EMG data set of each motor behavior. The algorithm was initiated with random nonnegative synergies (vectors whose dimensions were the same as the number of recorded muscles) and random coefficients. The algorithm then minimized the total reconstruction error by iterating a coefficient update step and a synergy update step based on multiplicative update rules. The criterion of convergence was set to be an increase of the reconstruction R^2 smaller than 10^{-4} for 20 consecutive iterations.

Table 1. *Summary of number of behavioral episodes collected*

| Experiment | Frog | Behavior | | | | | | | |
| | | Before transection | | | | After transection | | | |
		Jump	Swim	Kick	Step	Jump	Swim	Kick	Step
Intact vs. brain stem	*b1*	57	164 (321)	66	56 (85)	46 (47)	65 (129)	90	11 (18)
	b2	62	187 (373)	48	42 (66)	35	71 (137)	48	30 (42)
	b3	87	141 (296)	31		107	121 (244)	149	
Intact vs. medullary	*m1*	80 (83)	21 (84)	32				9	42 (83)
	m2	115 (125)	77 (424)	56	61 (117)			50	10 (11)
	m3	98	83 (362)	104	85 (161)			64	95 (137)
Intact vs. spinal	*s1*	85	56 (226)	9	7 (13)	Spinal reflex, 43			
	s2	178 (208)	100 (661)	79	47 (124)	Spinal reflex, 123			
	s3	68 (81)	20 (162)	26	56 (76)	Spinal reflex, 137			

Values are numbers of behavioral episodes collected. Numbers in parentheses refer to the total number of jump, swim, or step cycles observed. A single behavioral episode can involve multiple cycles of movement.

By application of NMF to each of the EMG data sets being compared, the dimensionality of each data set could be estimated by finding the number of muscle synergies needed for reconstructing the EMGs at a desired level of R^2. The dimensionality of each data set was used as an input to our next stage of analysis, which involved a simultaneous extraction of shared and specific synergies from multiple data sets (see below). A reasonable criterion for determining the number of muscle synergies needed for data reconstruction should ensure that this number can be chosen objectively and consistently across different animals. Here, following Cheung et al. (2009), the smallest number of synergies whose combination could explain >90% of total data variance was chosen as the appropriate number for a given data set.

Measuring the goodness of EMG reconstruction. The EMG patterns and their reconstructions from synergy combinations are multivariate time series. Thus a measure of the goodness of the reconstruction to the original EMGs must be defined by using multivariate measures of data variability. Here the total data variation (Mardia et al. 1979), defined as the trace of the covariance of the EMG-data matrix, was used to define a multivariate R^2 measure: $R^2 = 1 -$ SSE/SST, where SSE is the sum of the squared residuals and SST is the sum, over all EMG data points, of the difference of each EMG data point from the overall mean EMG. Thus the R^2 value above represents the fraction of total variation in the EMGs accounted for by the synergy reconstruction. This R^2 was used as a measure of the goodness of fit of the reconstruction to the data in the procedure of both separate and simultaneous synergy extractions, respectively.

Extracting shared and specific synergies. For this procedure, the EMG data sets collected before and after transection in each animal were concatenated together into a single data matrix. Following Cheung et al. (2005), a modified version of NMF was applied to the combined data set for finding synergies shared between the EMGs of the intact and reduced preparations, as well as synergies specific to each preparation. This simultaneous extraction of shared and specific synergies was made possible by the multiplicative update rules of the NMF. In this procedure, the dimensionality of each data set, assessed during the earlier step of separate EMG extractions (see above), was used to specify the dimensions of the synergy and coefficient matrices that initialized the algorithm. The final number of shared synergies was found by successively increasing the number of shared synergies extracted from 1, then 2, and so on, to the number at which the specific synergies for the two data sets became dissimilar in their structures. Readers are referred to Cheung et al. (2005) for details of how this analysis was implemented.

Quantifying Similarity of Synergies

We compared muscle synergies observed in the intact frog with those from the reduced preparations by quantifying their similarity by several measures. In the first stage of separate synergy extractions, we calculated the scalar product between all pairs of normalized synergy vectors (i.e., unit vectors) from the two synergy sets for the intact and reduced EMGs. Each synergy for the intact data set was matched to one for the reduced data set, which gave the highest scalar product between them. A synergy was regarded as shared between the intact and reduced data sets if their scalar product lay above a threshold value expected from chance, found by the following randomization procedure. We first generated 2,000 random synergies for each of the two data sets being compared; each random synergy consisted of random muscle weights sampled from the original EMG data for each muscle. We then calculated the scalar product of all possible pairs of random synergies from the two data sets (totaling $2,000 \times 2,000 = 4 \times 10^6$ pairs). The 95th percentile of this distribution of scalar product was then set to be our threshold scalar product value. With this criterion, we then counted the number of shared synergies (NSS) between the synergy sets for the intact and reduced conditions.

In the second stage of analysis in which shared and specific synergies were simultaneously extracted from the pooled EMGs, similarity between the two sets of synergies being compared (say, synergies for *data sets A* and *B*) was quantified by two different measures: *1*) synergy sharedness, defined as the ratio of the number of shared synergies discovered by the algorithm to the dimensionality of either synergy *set A* or *B*, whichever one is smaller, and *2*) the variance accounted for (VAF), defined as the fraction of total variance in *data set A* that could be accounted for by combination of synergies extracted from *data set B*. The mathematical definition of the VAF is the same as that of R^2. The first sharedness measure indicates the percentage of individual synergies that remain invariant after transection in the same animal. In contrast, the VAF measure indicates similarity in the sense of how well the whole synergy set extracted from one data set can explain another EMG data set. Thus the VAF is a more holistic measure of similarity because it takes the entire synergy set, rather than individual synergies, into account for the explanation of the total variance of another data set (Perreault et al. 2008).

To set a baseline VAF level for assessing the significance of the VAF values obtained, the EMG data set from which synergies were extracted for the fitting was randomly shuffled in time, independently in each muscle; random synergies were then extracted from this shuffled data set and fit to the unshuffled EMG data set to obtain a VAF value expected from chance. The paired *t*-test was applied to assess whether the VAFs obtained from the original, unshuffled EMGs were statistically higher than the VAFs from the shuffled EMGs. A statistically significant difference ($P < 0.05$), when the number of synergies is small, implies that the original data set possesses a low dimensionality, and the synergies extracted from the original data capture certain data structures of the unshuffled EMG data.

Finally, we attempted to identify the neural divisions that are minimally necessary for the expression of the synergies for each motor behavior observed in intact animals by comparing two groups of VAFs: one group obtained by fitting the synergies shared between the pre- and posttransection data sets (i.e., the shared synergies extracted from the pooled data set) to the pretransection EMG episodes, and the other group of VAFs acquired by fitting the pretransection synergies (i.e., the shared synergies extracted from the pooled data set plus intact-specific synergies) back to their own associated pretransection EMG episodes. We reasoned that if the subset of pretransection synergies observed even after transection (i.e., the shared synergies extracted from the pooled data set) could explain the variation of the pretransection data as much as the whole set of pretransection synergies could do, the neural divisions caudal to that transection were sufficient for the expression of that motor behavior. Fifteen different pairs of comparison conditions [VAFs at 3 transection levels $\times$ 2 conditions (pre- and posttransection conditions); $_6C_2 = 15$] were considered for each behavior. Two-way ANOVA with repeated measures (SAS version 9.2, SAS Institute, Cary, NC) was applied with Bonferroni correction ($\alpha = 0.05$). Correlation between repeated measurements from the same frog was accounted for in this statistic.

RESULTS

Electromyographic data (EMGs) were recorded from 12 or 13 muscles in a total of nine frogs, divided into three groups for three different comparisons: intact versus brain stem conditions ($n = 3$), intact versus medullary conditions ($n = 3$), and intact versus spinal conditions ($n = 3$). To maximize data variability, we collected data from all four major types of frog movements (jump, swim, kick, and step) in intact animals and from all manifested behaviors in the reduced preparations after transection. Two frogs (*b3* and *m1*) did not perform step in the

experiment. The number of episodes collected for each behavior is summarized in Table 1.

Observations of EMG Data Recorded Before and After Transection

In each of the behaviors studied, we observed distinctive groupings of muscle coactivations both before and after neural transection. Figure 2 shows representative examples of EMGs recorded during five cycles of swimming from *frog b2* before (Fig. 2*A*) and after (Fig. 2*B*) transection at rostral midbrain; during cycles of stepping from *frog m3* before (Fig. 2*C*) and after (Fig. 2*D*) transection at pons; and during reflexive movements from *frog s3*, elicited by cutaneous stimulations after spinalization (Fig. 2*E*). As shown in Fig. 2*A*, the EMGs of cycles of natural swimming in an intact animal can be divided into two phases, marked *a* and *b* in the figure and demarcated
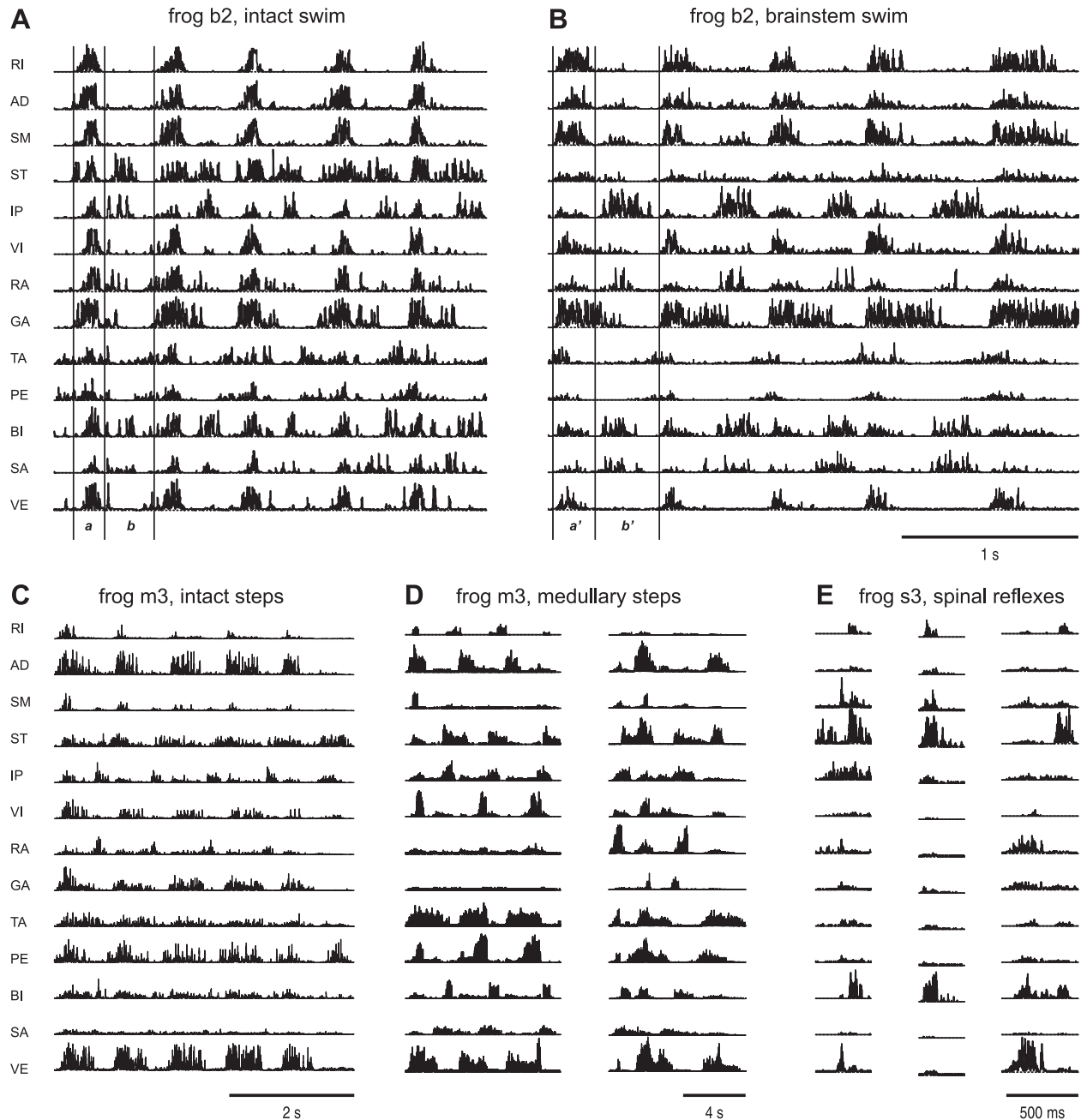

Fig. 2. Coactivation pattern across multiple muscles remained invariant after transection in each of these behavioral episodes. *A* and *B*: EMGs of swimming cycles recorded in the intact state (before transection) of *frog b2* (*A*) and under the brain stem condition of *frog b2* (*B*). *A* and *B* use the same timescale marked at the *bottom* of *B*. *C* and *D*: EMGs of stepping cycles recorded under the intact state of *frog m3* (*C*) and under the medullary condition of *frog m3* (*D*). The timescale is marked at the *bottom* of each panel. *E*: reflex episodes recorded in the spinal condition of *frog s3*. Note that the coactivations observed in *A*, such as those of semitendinosus (ST), iliopsoas (IP), and biceps femoris (BI), can still be seen even when the level of transection was lowered down from rostral midbrain in *B* with the reduced amplitude of ST activation, to rostral medulla in *C*, or to rostral spinal cord in *D*. The EMGs shown here were high-pass filtered and then rectified. In *A*, *a* and *b* indicate 2 phases in a cycle of swim; *a′* and *b′* in *B* refer to the 2 phases corresponding to phases *a* and *b* in *A*. RI, rectus internus; AD, adductor magnus; SM, semimembranosus; VI, vastus internus; RA, rectus anterior; GA, gastrocnemius; TA, tibialis anterior; PE, peroneus; SA, sartorius; VE, vastus externus.

by two vertical lines marking the burst onset and offset times of the hip extensor AD. The division of EMGs into phases is for ease of visual inspection. During *phase a*, almost all 13 muscles were activated; in *phase b*, ST, IP, RA, GA, TA, PE, BI, and SA were activated instead. The EMG episode evoked after transection can likewise be divided similarly into two phases, labeled *a′* and *b′* in Fig. 2*B*, corresponding to *phases a* and *b*, respectively, of a swim episode before transection in the same animal. The EMGs recorded from the brain stem preparation appeared to be characterized by activations of the same muscle groups involved in the EMGs of the intact preparation. For example, during *phase b′*, IP, RA, GA, BI, and SA were activated. Some muscles active during *phase b*, for example, ST, were active during *b′*, with a substantially reduced amplitude. In general, muscle activation groupings during swimming tended to remain invariant even after removal of telencephalic influences.

Similarly, visual inspection of other EMG examples suggests that synergistically activated muscle groups observed during stepping after transection at rostral medulla remained intact after transection at an even lower level, rostral to the spinal cord. During medullary steps (Fig. 2*D*), the extension phase during which almost all muscles were activated (except RA, GA, and SA) was followed by another phase during which mainly ST, IP, TA, BI, and SA activities were observed. After spinalization, the coactivations we have seen earlier in medullary steps, such as those of ST, IP and BI, can still be seen (Fig. 2*E*, *left* and *center*). Remarkably, this coactivation pattern of ST, IP, and BI was also observed in *frog b2* both in the intact (Fig. 2*A*, *phase b*) and brain stem (Fig. 2*B*, *phase b′*) conditions with the amplitude of ST reduced. The above observations motivated us to investigate similarities and differences between muscle synergies of the intact and reduced preparations. If muscle synergies extracted from EMG patterns obtained from reduced preparations show obvious similarities to the muscle synergies from intact behaving animals, then we may infer that those invariant synergies are expressed by neural circuitries caudal to the level of transection.

Data Dimensionalities Under Intact and Posttransection Conditions

We hypothesized that movements elicited before and after transection at any of the three levels we tested can be produced by a flexible combination of a small number of movement modules, or muscle synergies. To assess the number of muscle synergies present in each condition, the NMF algorithm was applied to the EMG data set of each behavior. For instance, Fig. 3, *A* and *B* show, for intact jump (i.e., jump observed before transection) and brain stem jump (i.e., jump observed in a brain stem preparation), respectively, plots of R^2 values (representing the fraction of total data variance explained by a combination of synergies) as a function of the number of synergies extracted. As the number of synergies extracted was increased from 1 to 8, the R^2 increased as well, as expected. In all behaviors before and after transection, ~90% of data variance in the original EMGs was explained by a combination of 3–6 synergies (Table 2; means ± SD across 3 animals for each condition). The fact that the number of synergies required for explaining a large fraction of EMG variance is

smaller than the dimensionalities of the EMG data (12 or 13) suggests that the data collected under both the intact and posttransection conditions possess low and comparable dimensionalities.

To verify the significance of the extracted synergies, the R^2 levels for the synergies extracted from the original data (solid curves in Fig. 3, *A* and *B*) were compared with the R^2 values for the synergies extracted from shuffled, structureless data (dashed curves). As can be seen, this comparison indicates that the R^2 values for 3–6 synergies extracted from the original data were significantly higher than those for the same numbers of synergies from the shuffled data. This R^2 difference was consistently observed in all behaviors of all nine animals. Since the EMG-amplitude distributions for each muscle were by definition the same in the original and shuffled data, the lower R^2 values for those synergies extracted from shuffled data imply that the structures of the synergies extracted from the original data reflect the spatial organization of muscle activities (d'Avella and Bizzi 2005).

We systematically assessed similarity between the two sets of synergies for behaviors before and after transection, respectively. The metric of similarity used was the NSS between two synergy sets, obtained from the number of significant scalar products between synergy pairs (see MATERIALS AND METHODS). For instance, Fig. 3, *C* and *D*, show, respectively, a set of four synergies for intact jump and a set of three synergies for brain stem jump. Note that the first three synergies for intact jump are also present in the set of synergies for brain stem jump. These shared synergies include *1*) a hip flexor synergy (with muscles IP, RA, and BI); *2*) a hip-knee extensor, knee flexor and ankle extensor synergy (RI, AD, SM, VI, GA, and VE); and *3*) a hip flexor and knee extensor synergy (VI, RA, BI, SA, and VE). Like jumping, in swimming we see relatively similar numbers of synergies preserved after transection. The first three synergies underlying intact swimming (Fig. 3*E*) were very similar to the first three synergies for brain stem swimming (Fig. 3*F*). The scalar products between those similar synergy pairs (shown on Fig. 3 as numbers placed in between the intact and posttransection synergies) were also much higher than those obtained by matching random vectors generated by random shuffling of synergy components ($P < 0.05$). Comparable levels of similarity between intact and posttransection synergies were observed in other animals and behaviors, as summarized in Table 2.

To this point, synergies were extracted from the data sets recorded from the intact and reduced preparations separately. This analysis was necessary for assessing the number of synergies underlying each EMG data set. However, as mentioned in Cheung et al. (2005), such an approach of analysis, though obvious, has several limitations and shortcomings. Thus in all subsequent analyses we present below, we follow the analytic approach outlined in Cheung et al. (2005) to extract shared and specific synergies from the data set that combines the pre- and posttransection EMGs together as a single data matrix for every behavior. This approach maximizes the number of shared muscle synergies discoverable without sacrificing the quality of data description in both data sets under consideration.

A frog b2, intact jump

B frog b2, brainstem jump

C frog b2, intact jump

D frog b2, brainstem jump

E frog b2, intact swim
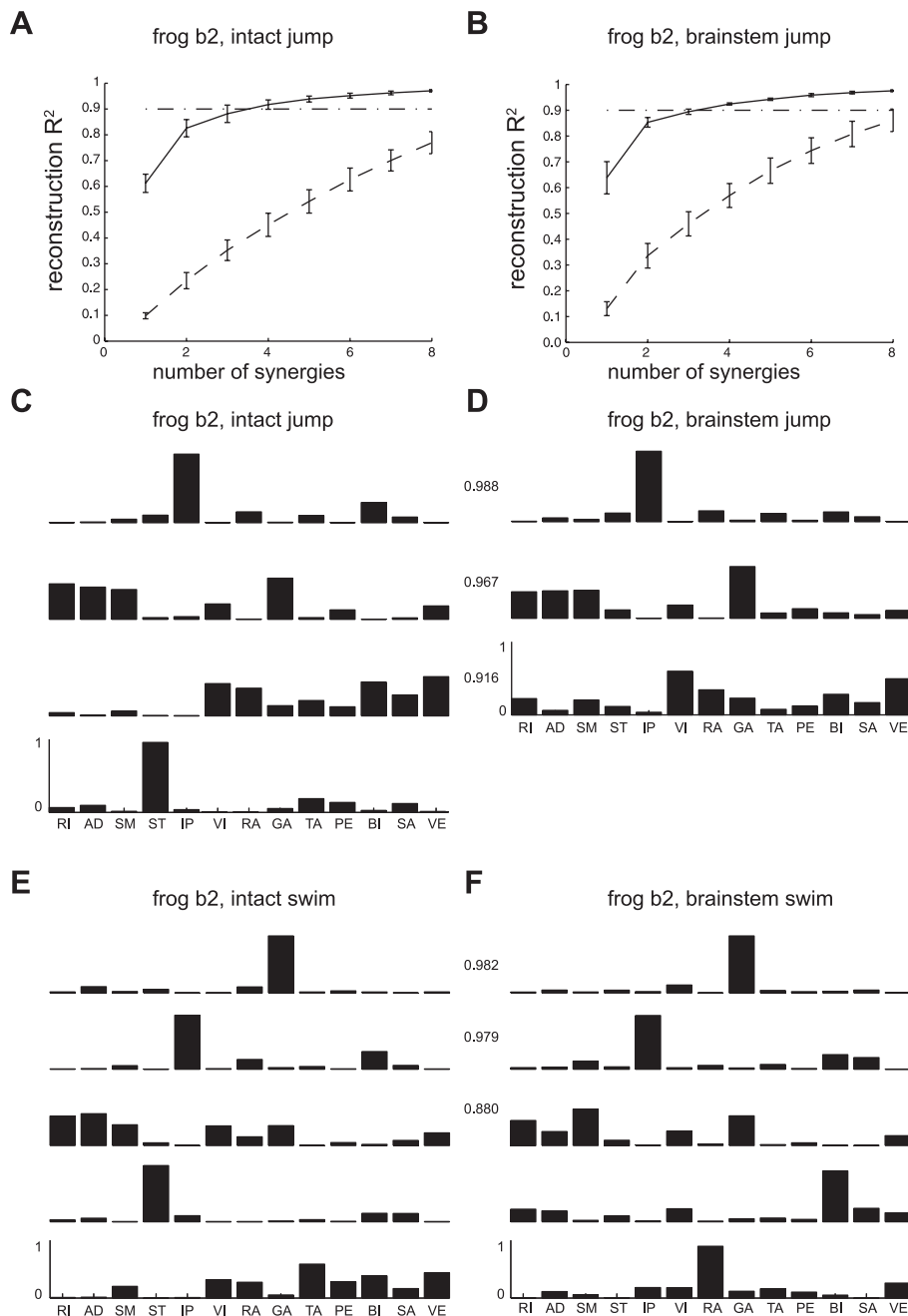
F frog b2, brainstem swim

Fig. 3. Example of separate extraction of synergies in intact vs. brain stem conditions. To estimate the number of synergies underlying each behavior, we separately extracted synergies from EMGs recorded before and after transection. A and B: the fraction of total EMG data variation, for jump in intact and brain stem conditions, respectively, displayed as a function of the number of extracted synergies. In each plot, the curves show that the percentage of data variance accounted for by synergy combinations (R^2; mean $\pm$ SD; $n = 20$) increased as the number of synergies extracted increased. The solid curves indicate how well a set of synergies extracted from the original EMG data set reconstructed the original data, while the dashed curves indicate how synergies extracted from the reshuffled EMGs reconstructed the original data. Note that the reconstruction R^2 values for original EMG signals were significantly higher than the R^2 values for reshuffled EMGs, suggesting that the extracted synergies capture structures in the original data set. C and D: sets of synergies separately extracted from EMGs collected during jump before (C) and after (D) transection in the same animal. The first 3 of 4 (C) synergies for natural jump were matched to 3 brain stem synergies that yielded maximal summation of scalar products between 2 synergy sets. E and F: sets of synergies separately extracted from EMGs collected during swims before (E) and after (F) transection in the same animal. The numbers between C and D and those between E and F are statistically significant scalar product values ($P < 0.05$).

Muscle Synergies in Intact vs. Brain Stem Conditions

Much like an intact frog, a brain stem frog (i.e., a frog behaving after transection at the rostral brain stem level; Fig. 1B) could also perform jumping, swimming, kicking, and stepping. This observation enables us to make a direct comparison of synergies for each behavior before and after CNS transection. The analytic approach we used allowed us to extract, simultaneously, three types of synergies from the data matrix composed of both pre- and posttransection EMGs: synergies common to both data sets, synergies specific to the pretransection EMGs, and synergies specific to the posttransection EMGs.

For all four behaviors, most of the synergies extracted by NMF were identified as synergies shared between the intact and brain stem EMGs (denoted by *sh* in Fig. 4, A–D). For instance, in the case of *frog b2*, there were 3 of 4 synergies shared between the two data sets (recorded before and after transection, respectively) for jump (Fig. 4A), 4 of 7 for swim (Fig. 4B), 4 of 5 for kick (Fig. 4C), and 4 of 5 for step (Fig. 4D). The synergies specific to pretransection or posttransection behaviors are respectively denoted by *INsp* or *TRsp* in Fig. 4, A–D. This observation of a higher number of shared synergies for each behavior compared with the NSS obtained earlier from separate extractions was consistent across all three animals, as summarized in Table 3.

After synergy extraction, similarity of synergies for both the intact and brain stem conditions in the same animal (counting both the shared and specific synergies found) was quantified. The sharedness measure we used indicates the ratio of the

Table 2. *Summary of separate extraction of synergies across three sets of comparison conditions*

Compared Preparation	Compared Behavior	N_{IN}	N_{TR}	NSS	R^2, %	
					Intact	Transected
IN vs. BS	INjump vs. TRjump	3.67 ± 0.58	3.67 ± 0.58	3.11 ± 0.18	91.1 ± 0.79	91.5 ± 1.08
	INswim vs. TRswim	5.00 ± 1.00	4.00 ± 1.00	2.92 ± 0.45	91.1 ± 0.75	91.4 ± 0.68
	INkick vs. TRkick	4.67 ± 0.58	5.00 ± 0.00	2.35 ± 0.89	91.5 ± 0.98	91.2 ± 0.76
	INstep vs. TRstep	5.00 ± 0.00	3.00 ± 0.00	2.22 ± 0.90	92.4 ± 1.20	91.4 ± 0.85
IN vs. MD	Jump vs. medullary	4.33 ± 0.58	6.67 ± 0.58	2.67 ± 1.00	91.7 ± 0.84	92.2 ± 0.56
	Swim vs. medullary	5.00 ± 0.00	6.67 ± 0.58	3.74 ± 0.68	91.5 ± 0.42	92.2 ± 0.56
	Kick vs. medullary	5.00 ± 1.00	6.67 ± 0.58	3.07 ± 1.09	91.3 ± 1.04	92.2 ± 0.56
	Step vs. medullary	5.00 ± 0.00	6.50 ± 0.71	2.74 ± 1.25	92.1 ± 0.42	92.3 ± 0.72
IN vs. SP	Jump vs. reflex	4.00 ± 1.00	3.33 ± 0.58	1.72 ± 0.31	90.9 ± 0.91	92.7 ± 1.25
	Swim vs. reflex	5.33 ± 1.15	3.33 ± 0.58	2.28 ± 0.63	90.7 ± 0.29	92.7 ± 1.20
	Kick vs. reflex	5.00 ± 0.00	3.33 ± 0.58	1.49 ± 1.21	92.1 ± 1.14	92.7 ± 1.20
	Step vs. reflex	5.33 ± 0.58	3.33 ± 0.58	2.42 ± 0.65	91.1 ± 0.40	92.7 ± 1.20

Values are means ± SD across animals in each comparison group. IN, intact preparation; BS, brain stem preparation; MD, medullary preparation; SP, spinal preparation; NSS, no. of shared synergies. "IN" behavior specifies behavior in intact preparation (e.g., INjump means jumps in intact animal); "TR" behavior specifies behavior in posttransection preparation (e.g., TRswim mean swims in preparation with neural transection); N_{IN}, no. of synergies in intact preparation; N_{TR}, no. of synergies in posttransection preparation.

number of shared synergies extracted to the dimensionality of either the pre- or posttransection EMGs, whichever one is smaller. A sharedness value of 0 means that the two synergy sets do not share any synergy; a value of 1 means that either the two sets are identical or one set is a subset of another. In all three frogs transected at rostral brain stem, the sharedness value for each of four behaviors is >0.9, as shown in Fig. 4*E* (means ± SD).

Furthermore, a large portion of pretransection- and posttransection-specific synergies of a single behavior were identified as shared synergies for other behaviors. For instance, the similarity between *INsp.1* of swims and *sh.4* of kicks in *frog b2* (Fig. 4, *B* and *C*) is above chance level (*P* < 0.05; see MATERIALS AND METHODS for details). In total, across the four motor behaviors, 8 of 12 and 5 of 7 intact- and posttransection-specific synergies seemed to be expressed by the brain stem and spinal circuitries and used to produce other movements (Fig. 4*F*).

The high values of sharedness (Fig. 4*E*) obtained when we compared the intact versus brain stem conditions and the observation that intact- and posttransection-specific synergies of one behavior appeared as shared synergies for other motor behaviors in an identical animal suggest that muscle synergies for generating movements under the intact condition persist even after a neural transection at rostral brain stem. Overall, the findings that the full repertoire of behaviors was observed after transection at rostral brain stem, and that synergies of movements under the intact condition were still found after transection, suggest that the neural circuitries within the brain stem and spinal cord are sufficient to activate and organize synergies for executing natural movements.

Muscle Synergies in Intact vs. Medullary Conditions

We proceeded to test whether neural circuitries within the medulla and spinal cord are sufficient to coordinate muscle synergies for producing behaviors found in an intact animal by lowering the level of transection to the caudal end of the pons to produce a medullary preparation (Fig. 1*C*). One major difference between brain stem and medullary frogs concerns their behavioral repertoire: while the brain stem frogs could perform all four major types of behaviors (jump, swim, kick,

and step), the medullary frogs could produce only kick-like defensive movements and disorganized steps. Some medullary behaviors were spontaneously generated without any external stimuli, probably as a result of the lack of supramedullary inhibition to the medulla and spinal cord. Because of such differences in behavioral repertoire between the intact and medullary frogs, we aimed at comparing the synergies of each individual behavior observed before transection with the synergies extracted from EMGs of all medullary behaviors combined. As in the previous section, we extracted synergies shared between the EMG data sets collected before and after transection (denoted by *sh* in Fig. 5, *A*–*D*) and those specific to intact- and posttransection data sets (*INsp* and *TRsp*, respectively, in Fig. 5, *A*–*D*) simultaneously.

Similar to the findings in intact versus brain stem conditions, an important portion of synergies for each behavior performed under intact conditions was kept invariant even after the supramedullary network was disconnected from the medullary and spinal circuitries. For instance, in the case of *frog m3*, there were 4 of 7 synergies that were found to be shared between the synergy sets for the intact jump and medullary behaviors (Fig. 5*A*), 4 of 8 for swim and medullary behaviors (Fig. 5*B*), 5 of 8 for kick and medullary behaviors (Fig. 5*C*), and 4 of 8 for step and medullary behaviors (Fig. 5*D*). These numbers of shared synergies (summarized in Table 3) resulted in sharedness values of >0.8 (Fig. 5*E*, means ± SD).

In addition, many intact- and posttransection-specific synergies of a certain motor behavior were identified as shared synergies for other behaviors. For example, the similarity between *INsp.1* for swim and *sh.4* for jump and that between *TRsp.1* for jump and *sh.4* of swim in *frog m3* (Fig. 5, *A* and *B*) were higher than that expected by chance (*P* < 0.05). Across the four behaviors, 9 of 11 intact-specific synergies and 21 of 31 posttransection-specific synergies appeared also as shared synergies for some other behaviors (Fig. 5*F*).

The high sharedness values and the large portion of specific synergies for one behavior used as shared synergies of other motor behaviors suggest that many intact synergies were kept invariant after transection at rostral medulla. Overall, we found that, after transection at rostral medulla, only a partial repertoire of behaviors was produced, but synergies found under
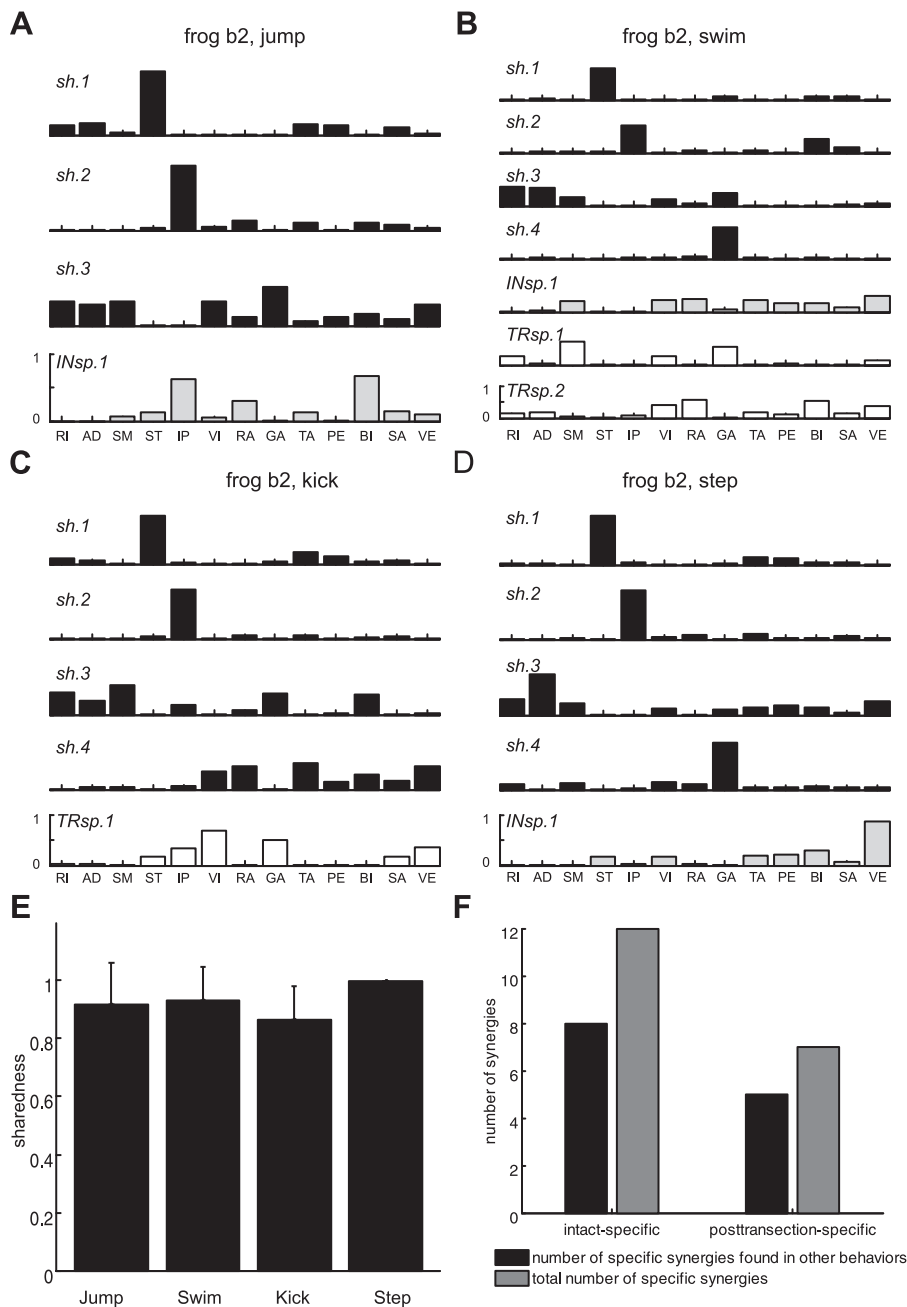
Fig. 4. Example of simultaneous extraction of shared and specific synergies in intact vs. brain stem conditions. Four sets of synergies for jump, swim, kick, and step, respectively, were extracted from the pooled EMG data sets recorded before and after transection in *frog b2*. In *A–D*, *sh* (black bars) refers to synergies shared between EMGs recorded in the intact and brain stem preparations, while *INsp* and *TRsp* (light gray and open bars, respectively) indicate individual intact-specific and posttransection-specific synergies. *A*: a set of 3 shared synergies and 1 intact EMG data set-specific synergy for jump. *B*: a set of 4 shared, 1 intact-specific, and 2 posttransection-specific synergies for swim. *C*: a set of 4 shared synergies and 1 posttransection-specific synergy for kick. *D*: a set of 4 shared synergies and 1 intact-specific synergy for step. Similarity between synergy sets was quantified by the sharedness measure. *E*: for each of 4 natural motor behaviors, sharedness (mean ± SD; $n = 3$) was defined as the average ratio of the number of shared synergies to the number of synergies that underlie the intact or brain stem EMGs, whichever number is smaller. High numbers of shared synergies resulted in high sharedness values (>0.8) in all 4 behaviors. *F*: across the 4 motor behaviors, in total, 8 of 12 and 5 of 7 intact- and posttransection-specific synergies appeared to be expressed by the brain stem and spinal circuitries and used to produce other movements. These findings support the idea that neural circuitries within the brain stem and spinal cord are sufficient to activate and express synergies for executing natural movements.

intact conditions were reasonably well preserved. These findings support the idea that the neural circuitries within and caudal to the medulla are not sufficient for triggering activations of muscle synergies to produce an entire repertoire of motor behaviors found in the intact state but enough for expressing the set of muscle synergies used for generating natural movements before transection.

Muscle Synergies in Intact vs. Spinal Conditions

Finally, we tested the degree to which the spinal cord is involved in expressing muscle synergies for generation of movements found in an intact animal. The level of neural transection was further lowered down to the caudal end of the fourth ventricle, just above the rostral end of the spinal cord, to create a spinal preparation. After spinalization, the animal could perform cutaneous reflexes but none of the four major types of behaviors observed in an intact frog. Thus we compared EMGs of each behavior in the intact state to those of spinal reflexes.

The results of the synergy analysis for comparing the intact versus spinal conditions confirm that most synergies found under the intact condition persisted after spinalization. For instance, in the case of *frog s3*, 4 of 6 synergies for intact jump (denoted by *sh*, Fig. 6*A*), 5 of 6 for swim (Fig. 6*B*), 4 of 5 for kick (Fig. 6*C*), and 4 of 6 for step (Fig. 6*D*) were ones found in spinal reflexes as well. The mean sharedness values were also reasonably high for all behaviors except jump (swim, kick, and step: ~0.8) but low in jump (~0.55) as shown in Fig. 6*E* (means ± SD). The portion of intact-specific synergies that appeared as shared synergies of other motor behaviors was also

Table 3. *Summary of estimated number of shared and data set-specific synergies across three comparison conditions*

Compared Preparation	Compared Behavior	N_{IN}	N_{TR}	N_{sh}	N_{spIN}	N_{spTR}	R^2, %	
							Intact	Transected
IN vs. BS	INjump vs. TRjump	3.67 ± 0.58	3.67 ± 0.58	3.00 ± 0.00	0.67 ± 0.58	0.67 ± 0.58	89.5 ± 2.20	90.5 ± 1.06
	INswim vs. TRswim	5.33 ± 0.58	4.33 ± 1.53	3.67 ± 0.58	1.67 ± 1.15	0.67 ± 1.15	88.2 ± 1.00	91.5 ± 0.56
	INkick vs. TRkick	4.67 ± 0.58	5.00 ± 0.00	4.00 ± 0.00	0.67 ± 0.58	1.00 ± 0.00	90.5 ± 1.04	90.7 ± 0.38
	INstep vs. TRstep	5.00 ± 0.00	3.50 ± 0.71	3.50 ± 0.71	1.50 ± 0.71	0.00 ± 0.00	88.4 ± 2.34	93.4 ± 2.59
IN vs. MD	Jump vs. medullary	4.33 ± 0.58	7.00 ± 0.00	4.00 ± 1.00	0.33 ± 0.58	3.00 ± 1.00	90.7 ± 1.04	89.4 ± 1.02
	Swim vs. medullary	5.33 ± 0.58	6.67 ± 0.58	4.33 ± 0.58	1.00 ± 0.00	2.33 ± 0.58	89.8 ± 1.00	92.0 ± 0.85
	Kick vs. medullary	5.00 ± 1.00	7.00 ± 1.00	3.67 ± 1.53	1.33 ± 1.53	3.33 ± 1.15	89.6 ± 0.67	92.5 ± 1.69
	Step vs. medullary	5.00 ± 0.00	6.50 ± 0.71	3.50 ± 0.71	1.50 ± 0.71	3.00 ± 0.00	91.4 ± 0.50	92.1 ± 0.74
IN vs. SP	Jump vs. reflex	4.00 ± 1.00	4.00 ± 1.00	2.33 ± 1.53	1.67 ± 0.58	1.67 ± 0.58	90.0 ± 1.88	90.5 ± 1.30
	Swim vs. reflex	5.33 ± 1.15	4.00 ± 1.00	3.33 ± 1.53	2.00 ± 1.00	0.67 ± 0.58	89.3 ± 0.76	89.5 ± 4.88
	Kick vs. reflex	5.00 ± 0.00	3.33 ± 0.58	2.67 ± 1.53	2.33 ± 1.53	0.67 ± 1.15	91.8 ± 1.34	91.6 ± 3.06
	Step vs. reflex	5.33 ± 0.58	3.67 ± 0.58	3.00 ± 1.00	2.33 ± 0.58	0.67 ± 0.58	90.5 ± 0.60	92.6 ± 0.48

Values are means $\pm$ SD across animals in each comparison group. IN, intact preparation; BS, brain stem preparation; MD, medullary preparation; SP, spinal preparation. "IN" behavior specifies behavior in intact preparation (e.g., INjump means jumps in intact animal); "TR" behavior specifies behavior in posttransection preparation (e.g., TRswim means swims in preparation with neural transection); N_{IN}, number of synergies in intact preparation; N_{TR}, number of synergies in posttransection preparation; N_{sh}, number of shared synergies; N_{spIN}, number of intact data-specific synergies; N_{spTR}, number of posttransection data-specific synergies.

low (9 of 25, 36% in Fig. 6*F*), compared with the values in intact vs. brain stem (66.7%, Fig. 4*F*) and intact vs. medullary conditions (81.8%, Fig. 5*F*), respectively. All together, these results suggest that spinal circuitries are involved in expressing muscle synergies for jump, swim, kick, and step, but the spinal cord alone does not appear to be sufficient for the expression of the entire set of synergies utilized for natural behaviors.

Localizing Muscle Synergies

As the last step of our analysis, we sought to clarify the minimal set of neural divisions necessary for the expression of synergies used in each motor behavior observed before transection. We reasoned that if the divisions above a transection level are critical for either activating or organizing the synergy(ies) for a behavior, the set of synergies found to be shared between the pre- and posttransection data sets should be inadequate for explaining the pretransection EMGs. The minimal set of neural divisions necessary can then be located by comparing the VAFs obtained by fitting the intact synergies to the intact data with the VAFs obtained by fitting the shared synergies to the intact data; the most rostral transection that results in a significant drop of the latter VAF compared with the former demarcates the rostral boundary of this minimal set. In addition, we assume that a similar drop in the sharedness value, another similarity measure we utilized above, could indicate the boundary of the minimal set of the neural divisions as well.

We show the results of this analysis in Fig. 7. Figure 7, *A*–*D*, show a summary of the mean (each bar) and distribution (with each asterisk denoting the value from each animal) of sharedness values indicating the degree to which individual synergies were common in pre- and posttransection synergy sets for each behavior. The sharedness value under an intact condition, when all neural systems were intact, should by definition be 1. The bar labeled "caudal to brain stem" in each panel of Fig. 7, for instance, indicates the mean of sharedness values between the intact and brain stem synergies across the three animals. Because of the relatively small number of animals studied in each comparison ($n = 2$ or 3), we chose not to perform any statistical test on this analysis, but Fig. 7, *A*–*D*, consistently

demonstrate that >70% of the synergies in intact animals across four behaviors were preserved after transection at the level of rostral medulla.

Figure 7, *E*–*H*, show the other similarity measure we adopted, the VAF values. The bars labeled "intact" indicate VAFs obtained by fitting the intact synergies back to their own associated intact EMG data sets; these VAFs may be regarded as control values against which the other VAFs were compared. Bars labeled "caudal to brain stem" refer to the VAFs obtained by fitting the synergies shared between the intact and brain stem data sets to the intact data; "caudal to medulla" refers to fitting synergies shared between the intact and medullary data sets to the intact data; and "caudal to spinal cord" refers to fitting synergies shared between the intact and spinal data sets to the intact data. Remarkably, in the cases of jump and kick (Fig. 7, *E* and *G*), even when the level of transection was lowered to the spinal-medullary junction, the VAFs obtained by fitting spinal synergies did not significantly decrease when compared against VAFs obtained by fitting intact synergies (2-way ANOVA with repeated measures between pre- and posttransection and 3 different transection conditions, adjusted $P > 0.05$). This finding implies that spinal circuitries are involved in expressing muscle synergies used in jump and kick episodes. In contrast, in the case of swim and step (Fig. 7, *F* and *H*), as the level of transection was lowered to the spinal-medullary junction, the VAF values decreased significantly (2-way ANOVA with repeated measures, adjusted $P < 0.05$). These results suggest that supraspinal circuits within the brain stem are involved in expressing some of the swimming and stepping muscle synergies. To summarize, our findings in this analysis support the idea that neural circuitries in the spinal cord are the key neural division that express muscle synergies underlying jump and kick, but supraspinal circuits within the brain stem are crucial in either activating and/or organizing selected synergies for swimming and stepping.

DISCUSSION

We compared muscle synergies underlying frog motor behaviors observed before and after CNS transection at different levels to test the hypothesis that neural circuitries within the
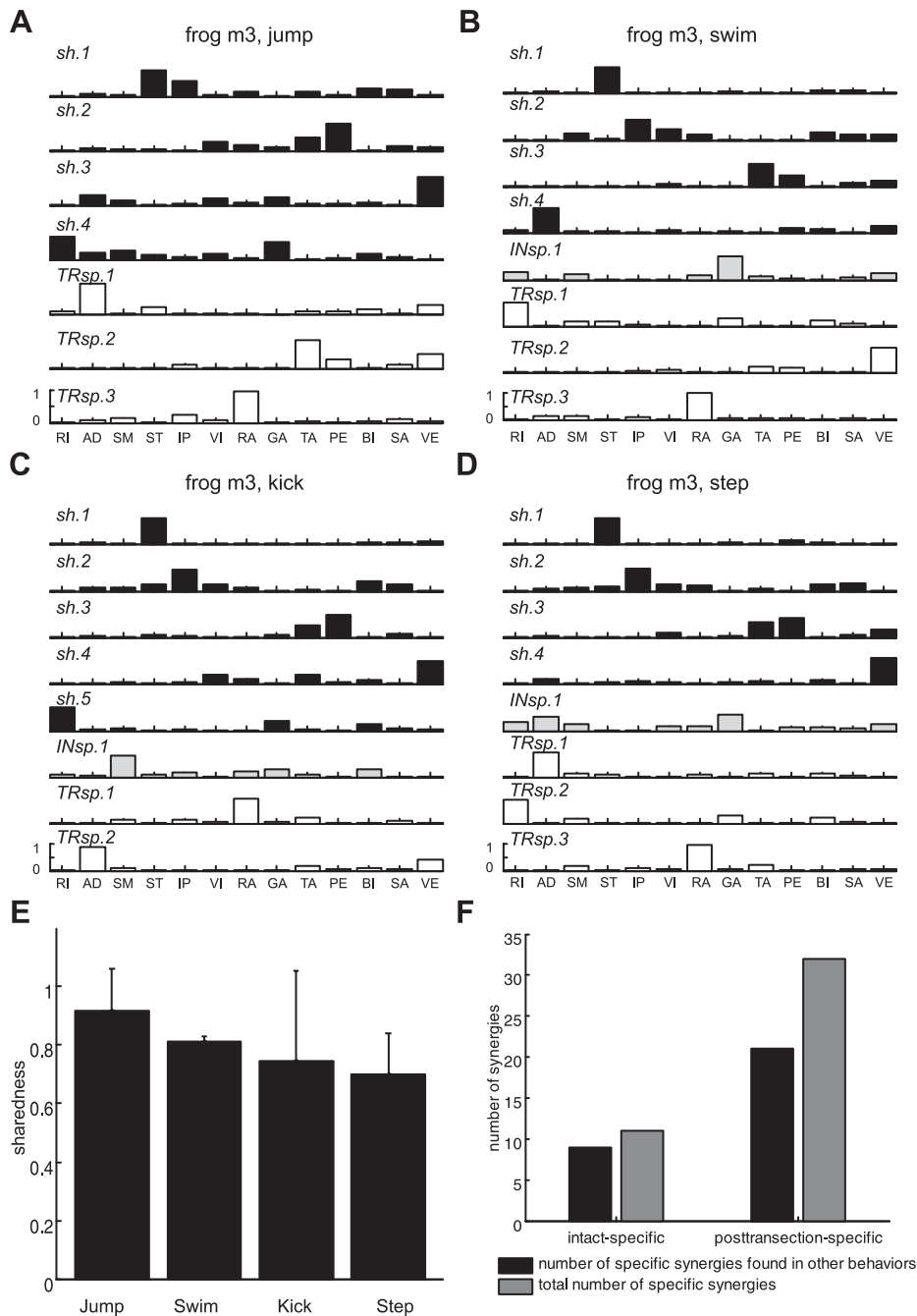
Fig. 5. Example of simultaneous extraction of shared and specific synergies in intact vs. medullary conditions. *A–D* are analogous to *A–D* in Fig. 4. High sharedness values (*E*) found in all 4 behaviors (~0.8) and many intact- and posttransection-specific synergies of a certain motor behavior identified as shared synergies for other behaviors (*F*) were observed, which suggests that the neural circuitries within and caudal to the medulla are sufficient for expressing the set of muscle synergies used for generating natural movements.

brain stem and spinal cord express muscle synergies used for execution of natural motor behaviors. Transections at rostral midbrain, rostral medulla, and rostral spinal cord were performed. While brain stem frogs produced a repertoire of behaviors similar to that of intact animals, medullary and spinal animals could express only a limited set of motor behaviors. This suggests that supramedullary circuitries are necessary for the production of the entire range of motor behaviors. The NMF algorithm was then applied to EMG data sets. We found that the muscle synergies before and after medullary transection were similar for all four behaviors and synergies before and after spinalization were similar for two of four behaviors (jump and kick). Overall, our results suggest that the synergies used for frog natural behaviors are organized

within the medulla and spinal cord; descending commands from the midbrain and telencephalon activate and coordinate these synergies appropriately for the production of diverse movements.

Neural Circuitries That Express Muscle Synergies

Our data support the idea that the brain stem and spinal cord circuitries express the muscle synergies whose linear combination can generate diverse movements in intact animals. All brain stem frogs could perform the four major motor behaviors (jump, swim, kick, and step), enabling us to compare the pre- and posttransection EMGs for each of the four behaviors. High values of the similarity measures we used for synergy comparison (Fig. 4*E*) were observed in all four behaviors, demonstrat-
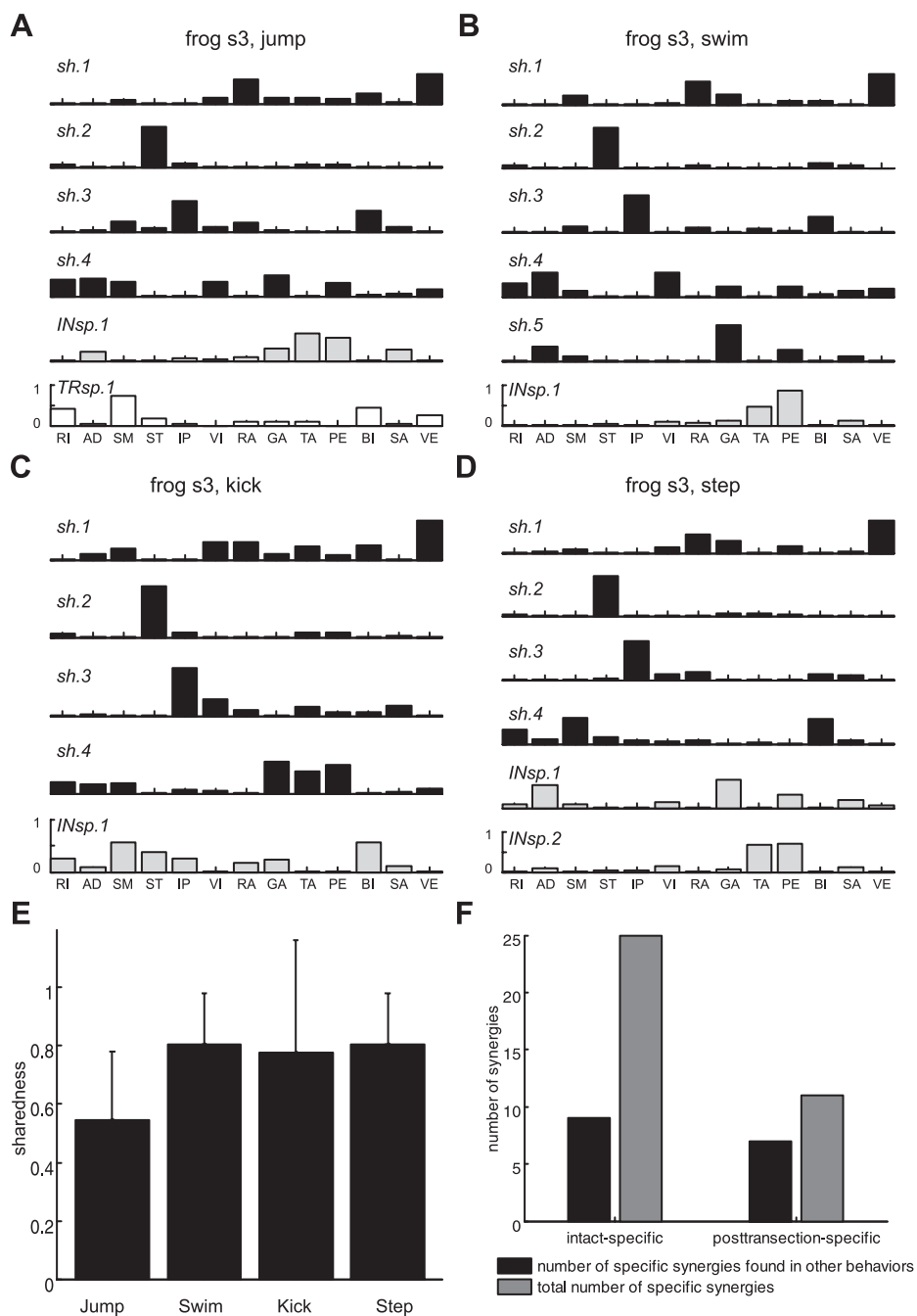
Fig. 6. Example of simultaneous extraction of synergies in intact vs. spinal conditions. *A–D* here are analogous to *A–D* in Figs. 4 and 5. High sharedness values were found in kick, swim, and step (~0.8) but not in jump (~ 0.55) (*E*). In addition, only 36% (9 of 25) intact-specific synergies of a single motor behavior were observed in other movements as shared synergies (*F*). These results suggest that many of the synergies for natural behaviors are organized within the spinal cord, but the supraspinal circuits may contribute to the expression of synergies utilized for natural behaviors.

ing that the synergies underlying those movements in intact animals remained invariant after transection. This result implies that the frog telencephalon is not required for activating and structuring the synergies necessary for generating movement in the intact state. As shown in Fig. 7, *E–H*, in two of the four behaviors examined a large portion of data variance in the intact EMGs could be accounted for by synergies shared between the data sets for the intact and reduced (brain stem, medullary, or spinalized) preparations. This analysis offers additional support for the hypothesis that most muscle synergies observed during natural behaviors are low-level motor controllers for whose expressions the brain stem and spinal cord are sufficient. The descending motor systems may then function to sculpt the activations of the synergies properly by

interacting with the brain stem and spinal circuits, so that every behavior can be executed properly.

This conclusion of ours is consistent with that of Hart and Giszter (2004), in the sense that their data also support a modular composition of frog motor behaviors, generated by a small collection of movement modules (note that their "brainstem frogs" correspond to our medullary frogs). In Hart and Giszter (2004), a comparison of medullary and spinal movement modules reveals that the internal structures of the two sets of movement modules are similar, but each of their medullary modules contains activations from a smaller number of muscles than their spinal modules. This observation is not inconsistent with our finding. In fact, our medullary EMG data sets did require a slightly higher number of synergies (6 or 7)
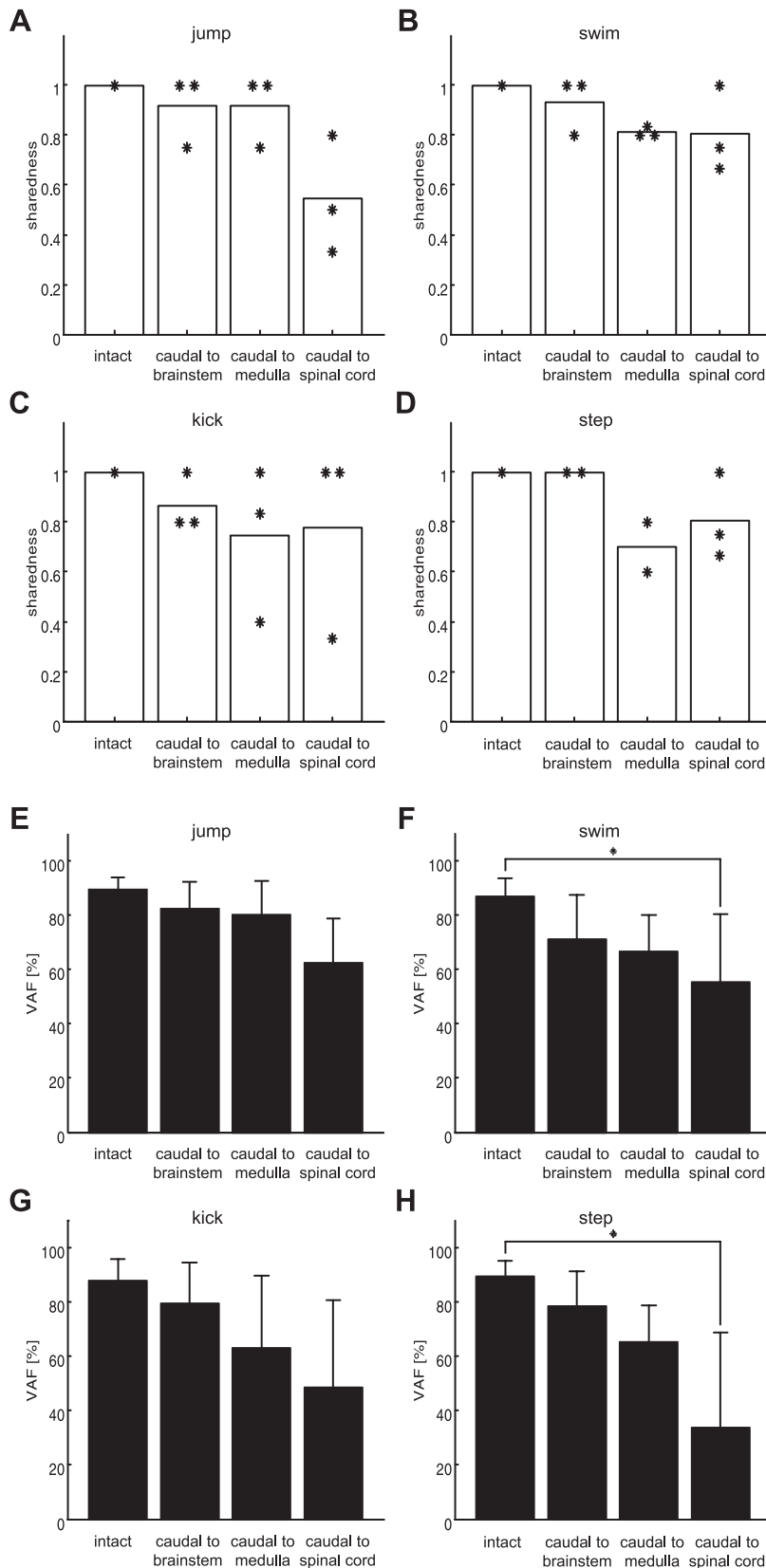
Fig. 7. Summary of similarity measures of muscle synergies between pre- and posttransection. A–D show the mean (each bar) and distribution of sharedness values, with each asterisk denoting the value from each animal in 4 intact behaviors [jump (A), swim (B), kick (C), and step (D)]. The sharedness values indicate the degree to which individual synergies were common in pre- and posttransection for each behavior. For instance, the bar labeled "caudal to brain stem" shown in A implies that, on average, 92% of synergies for jump were found in brain stem preparations across the 3 animals. A–D demonstrate that >70% of the synergies in intact animals were preserved after transection at the level of rostral medulla across 4 behaviors. E–H show the mean variance of EMG episodes in 4 intact behaviors [jump (E), swim (F), kick (G), and step (H)] accounted for by synergies shared between the pre- and posttransection data sets [variance accounted for (VAF); means ± SD]. For instance, the bar labeled "caudal to brain stem" in F refers to how well synergies shared between pre- and posttransection at rostral brain stem could explain the variance of swim EMGs in intact animals (see main text for full description). In the cases of jump and kick, even when the level of transection was lowered to rostral spinal cord the VAFs obtained (bars labeled "caudal to spinal cord" in E and G) did not significantly decrease even when compared against the intact VAFs (2-way ANOVA with repeated measures, adjusted $P > 0.05$). This finding implies that the spinal circuitries are sufficient for expressing muscle synergies for jump and kick. In contrast, in the case of swim and step (F and H), as the level of transection was lowered to rostral spinal cord the VAF values significantly decreased (2-way ANOVA with repeated measures, adjusted $P < 0.05$), suggesting that supraspinal circuits within the brain stem are involved in expressing at least some of the swim and step muscle synergies.

than our spinal data set for equivalent levels of data description; because of the nonnegativity constraints of NMF, the more synergies one extracts from a data set, the sparser the composition of each synergy becomes. Assuming that the synergies returned by NMF in our study do correspond to physiological entities, the higher number of synergies needed for the medullary EMGs may be due to a lack of inhibitory descending inputs from the supramedullary circuitries, result-

ing in the expression of other synergies not normally recruited during execution of natural movement.

The known anatomy of the brain stem and spinal cord circuitries also supports the idea that the brain stem and spinal cord are sufficient for expressing muscle synergies in the frog. For example, the divergent projection patterns of some spinal interneuronal systems may coordinate different motoneuronal pools, coactivating them as muscle synergies (Jankowska 1992, 2001; Tantisira et al. 1996; Tresch and Jarc 2009). Many reticulospinal and vestibulospinal fibers in the frog establish monosynaptic connections with lumbar motoneurons (Barale et al. 1971; Cruce 1974; Magherini et al. 1974; Shapovalov 1975), suggesting that the neural circuitries in the brain stem, in addition to those within the spinal cord, may also be the neural substrates of some of the synergies utilized for generating natural motor behaviors (Roh 2008).

Other studies from the field of postural control have also suggested that muscle synergies are organized by brain stem and spinal cord circuitries. There have been experimental results suggesting that supraspinal connections to the spinal cord are essential for postural maintenance in the cat (Lockhart and Ting 2007). Decerebrated cats are able to walk and produce righting responses (Deliagina et al. 2007), suggesting that the cerebral cortex is not required for postural orientation. In contrast, animals with complete spinal cord transection can walk but do not produce directionally specific postural responses (Macpherson and Fung 1999), implying that the brain stem must be involved in estimating task-level variables critical for postural control. The fact that robust and directionally selective muscle tuning is present without the cerebral cortices in the cat also supports a potentially important role for the brain stem and spinal cord circuitries in mediating directional tuning of muscles (Honeycutt et al. 2009). Experimental evidence from studies in postural and movement control during reaching in the cat suggests that the reticulospinal neurons play a role in encoding muscle synergies in postural adjustments during a voluntary task (Schepens and Drew 2004) as well.

A recent study on voluntary actions after cortical stroke in humans demonstrates that the muscular compositions of the synergies for both the unaffected and the stroke-affected arms are similar to each other despite differences in motor performance between the two arms (Cheung et al. 2009). If neural circuitries within the motor cortex are involved in organizing muscle synergies used for production of normal movement, the internal structures of synergies should be modified after stroke, but the results presented in that study do not seem to follow this scenario. The finding of this human study agrees generally with our conclusion that the function of descending cortical signals may be to select and flexibly activate muscle synergies organized by the neural networks within the brain stem and spinal cord.

Role of Primary Motor Cortex

The primary motor cortex (M1) has been proposed as a candidate brain region that organizes muscle synergies. Electrophysiological and anatomic studies in the cat have shown that many corticospinal neurons extend divergent branches in the spinal cord, innervating several different motoneuronal pools (Futami et al. 1979; Li and Martin 2002; Shinoda et al. 1976, 1986). Krouchev and colleagues (2006) demonstrated

that in cat locomotion different subpopulations of motor cortical neurons, activated sequentially during the step cycle, may regulate the timing of muscle synergy activations throughout the step cycle (Drew et al. 2008). In nonhuman primates, the divergent projection of individual corticospinal axons to motoneurons of multiple muscles has been demonstrated (Shinoda et al. 1981). In humans, a comparison of kinematic synergies evoked by transcranial magnetic stimulation (TMS) to kinematic synergies of voluntary finger movements shows that there is dimensionality reduction in TMS-elicited movements, which implies that corticomotoneuronal cells coordinate hand muscles in a way that results in reduction in movement dimensions (Gentner and Classen 2006). The studies summarized above together suggest that M1 could also be the region organizing muscle synergies for natural behaviors.

We think our conclusion here, derived from experiments using a lower vertebrate, that synergies are structured by the brain stem and/or spinal cord networks is not inconsistent with the view that in mammals the motor cortex may play a role also in synergy organization. In fact, a recent anatomic study (Rathelot and Strick 2009) has shown that the M1 of the monkey contains two subdivisions—a rostral, "old" division that sends descending fibers primarily to the spinal interneurons and a caudal, "new" division that innervates the motoneurons directly. It is conceivable that the "old" M1 generates movements by modulating synergies organized downstream (see also Yakovenko et al. 2011), while the "new" M1 organizes synergies for more agile movements peculiar to higher primates and humans. How the cortex, brain stem, and spinal cord cooperate to execute movements through combining these synergies organized in different regions would require further studies for clarification.

Data Set-Specific Synergies

In this study we have found that some of the muscle synergies are shared between several different behaviors. For example, shared synergies 1 and 2 (*sh.1* and *sh.2*) for jump of *frog b2* were observed also in swim, kick, and step in the same animal (Fig. 4, *A–D*); shared synergy 3 (*sh.3*) for swim of *frog b2* is similar to *sh.3* for kick and *sh.3* for step of the same animal (Fig. 4, *B–D*). This finding is consistent with the conclusion of our previous study (d'Avella and Bizzi 2005) that describes how some synergies may be shared between multiple behaviors.

Similarly, we found that some of the synergies specific to either the pre- or posttransection state for one behavior were similar to synergies identified as shared synergies for other motor behaviors. Not all intact- or posttransection-specific synergies, however, were identified as shared synergies of other behaviors. For instance, *TRsp.1* for kicks and *INsp.1* for step in *frog b2* (Fig. 4, *C* and *D*) were not matched to any shared synergy of the same frog. Across the three comparisons, on average 54% of intact-specific synergies and 66% of posttransection-specific synergies were identified also as synergies shared between pre- and posttransection states for other behaviors. However, for the intact versus spinal conditions specifically, only 36% of the intact-specific synergies were matched to other shared synergies, a percentage substantially lower than those for the intact versus brain stem and intact versus medullary conditions. This finding is consistent with our analysis

summarized in Fig. 7 that the spinal cord alone is not sufficient for the expression of certain muscle synergies required for locomotor behaviors such as swim and step.

We speculate that a potential role of the higher-level motor areas such as the M1 is to select and activate, for any given task, an appropriate subset of synergies within the pool of available synergies organized by the lower-level circuitries such as those in the spinal cord. In our experiment, it is possible that after transection the lack of appropriate descending commands for one behavior resulted in the faulty recruitment of synergies normally used for another behavior, thus explaining how the specific synergies for one behavior could emerge as the shared synergies for another behavior, as we have noted above. This possibility may be especially relevant to the animals receiving a medullary transection, after which their motor behaviors appeared to be more disorganized.

Methodological Considerations

We have quantified the similarity of two sets of synergies found before and after transection in two different ways: one as sharedness values reflecting similarity between individual synergies and the other as VAFs reflecting similarity between two sets of synergies. In intact versus brain stem and intact versus medullary conditions, both sharedness and VAFs were high (>70%) and comparably similar (Fig. 7). In contrast, in intact versus spinal conditions there were discrepancies between the two similarity measures: the sharedness value for jump was <60%, lower than the ~70% VAF; the sharedness values for swim, kick, and step were all ~80%, but the VAF values were ~55%, ~50%, and ~30%, respectively. This observation indicates that these two different ways for quantifying synergy similarity may reflect different aspects of similarity of the two synergy sets. We think that our results caution against solely relying on the absolute number of synergies common to two data sets for quantifying similarity of the synergy sets, which some previous studies have adopted in their synergy analysis (Cheung et al. 2009).

We have focused on comparing muscle synergies between pre- and posttransection states to address the question of which regions of the CNS are involved in expressing muscle synergies. This study, however, does not include any thorough analysis of movement kinematics. But we did observe that the same behavior was executed differently after transection. For example, we saw that the speed of movement in the brain stem preparation was in general slower than that in the intact animal. As shown in Fig. 2, *A* and *B*, for *frog b2*, the average duration of every swim cycle before transection (484.8 ± 31.2 ms, mean ± SD) was ~1.4 times shorter than that observed after transection (656.0 ± 101.4 ms). Similarly, the medullary preparation also showed lower speed of movement than the intact animal: in *frog m3* the average duration of a step cycle before transection was ~1.8 times shorter than that after transection (Fig. 2, *C* and *D*). Such differences between the pre- and posttransection kinematics, though not exhaustively documented in the present study, reinforce our proposition that the higher-level motor areas contribute to movement execution by sculpting the activations of the muscle synergies appropriately for the proper execution of each task.

To conclude, the present study sought to investigate the neural divisions responsible for organizing muscle synergies observed in movements of intact animals by comparing muscle synergies found before and after transection of the neuraxis at different levels. We maximized the variation of movement patterns analyzed by recording from four major types of behaviors. Our results support the idea that the neural circuitries within the brain stem and spinal cord are sufficient for the activation and/or organization of muscle synergies seen in normal motor patterns, although the supramedullary circuitries are needed for coordinating these synergies for the proper execution of different behaviors.

REFERENCES

Barale F, Corvaja N, Pompeiano O. Vestibular influences on postural activity in frog. *Arch Ital Biol* 109: 27–36, 1971.

Bizzi E, Cheung VC, d'Avella A, Saltiel P, Tresch M. Combining modules for movement. *Brain Res Rev* 57: 125–133, 2008.

Bizzi E, Mussa-Ivaldi FA, Giszter SF. Computations underlying the execution of movement: a biological perspective. *Science* 253: 287–291, 1991.

Cajigas-González I. *Linear Control Model of the Spinal Processing of Descending Neural Signals* (Master's thesis). Cambridge, MA: Massachusetts Inst. of Technology, 2003.

Cappellini G, Ivanenko YP, Poppele RE, Lacquaniti F. Motor patterns in human walking and running. *J Neurophysiol* 95: 3426–3437, 2006.

Cheng J, Stein RB, Jovanovic K, Yoshida K, Bennett DJ, Han Y. Identification, localization, and modulation of neural networks for walking in the mudpuppy (*Necturus maculatus*) spinal cord. *J Neurosci* 18: 4295–4304, 1998.

Cheung VC, d'Avella A, Tresch MC, Bizzi E. Central and sensory contributions to the activation and organization of muscle synergies during natural motor behaviors. *J Neurosci* 25: 6419–6434, 2005.

Cheung VC, Piron L, Agostini M, Silvoni S, Turolla A, Bizzi E. Stability of muscle synergies for voluntary actions after cortical stroke in humans. *Proc Natl Acad Sci USA* 106: 19563–19568, 2009.

Clark DJ, Ting LH, Zajac FE, Neptune RR, Kautz SA. Merging of healthy motor modules predicts reduced locomotor performance and muscle coordination complexity post-stroke. *J Neurophysiol* 103: 844–857, 2010.

Cruce WL. A supraspinal monosynaptic input to hindlimb motoneurons in lumbar spinal cord of the frog, *Rana catesbeiana*. *J Neurophysiol* 37: 691–704, 1974.

d'Avella A, Saltiel P, Bizzi E. Combinations of muscle synergies in the construction of a natural motor behavior. *Nat Neurosci* 6: 300–308, 2003.

d'Avella A, Bizzi E. Shared and specific muscle synergies in natural motor behaviors. *Proc Natl Acad Sci USA* 102: 3076–3081, 2005.

d'Avella A, Portone A, Fernandez L, Lacquaniti F. Control of fast-reaching movements by muscle synergy combinations. *J Neurosci* 26: 7791–7810, 2006.

Deliagina TG, Zelenin PV, Beloozerova IN, Orlovsky GN. Nervous mechanisms controlling body posture. *Physiol Behav* 92: 148–154, 2007.

Drew T, Kalaska J, Krouchev N. Muscle synergies during locomotion in the cat: a model for motor cortex control. *J Physiol* 586: 1239–1245, 2008.

Ecker A. *The Anatomy of the Frog* (Haslam G, translator). Amsterdam: Asher, 1971.

Fetz EE, Perlmutter SI, Prut Y. Functions of mammalian spinal interneurons during movement. *Curr Opin Neurobiol* 10: 699–707, 2000.

Futami T, Shinoda Y, Yokota J. Spinal axon collaterals of corticospinal neurons identified by intracellular injection of horseradish peroxide. *Brain Res* 164: 279–284, 1979.

Gentner R, Classen J. Modular organization of finger movements by the human central nervous system. *Neuron* 52: 731–742, 2006.

Giszter SF, Mussa-Ivaldi FA, Bizzi E. Convergent force fields organized in the frog's spinal cord. *J Neurosci* 13: 467–491, 1993.

Giszter SF, Kargo WJ. Conserved temporal dynamics and vector superposition of primitives in frog wiping reflexes during spontaneous extensor deletions. *Neurocomputing* 32–33: 775–783, 2000.

Grillner S. Neurobiological bases of rhythmic motor acts in vertebrates. *Science* 228: 143–149, 1985.

Hart CB, Giszter SF. Modular premotor drives and unit bursts as primitives for frog motor behaviors. *J Neurosci* 24: 5269–5282, 2004.

Hart CB, Giszter SF. A neural basis for motor primitives in the spinal cord. *J Neurosci* 30: 1322–1336, 2010.

Honeycutt CF, Gottschall JS, Nichols TR. Electromyographic responses from the hindlimb muscles of the decerebrate cat to horizontal support surface perturbations. *J Neurophysiol* 101: 2751–2761, 2009.

Ivanenko YP, Cappellini G, Dominici N, Poppele RE, Lacquaniti F. Modular control of limb movements during human locomotion. *J Neurosci* 27: 11149–11161, 2007.

Jankowska E. Interneuronal relay in spinal pathways from proprioceptors. *Prog Neurobiol* 38: 335–378, 1992.

Jankowska E. Spinal interneuronal systems: identification, multifunctional character and reconfigurations in mammals. *J Physiol* 533: 31–40, 2001.

Kargo WJ, Giszter SF. Afferent roles in hindlimb wipe-reflex trajectories: free-limb kinematics and motor patterns. *J Neurophysiol* 83: 1480–1501, 2000a.

Kargo WJ, Giszter SF. Rapid correction of aimed movements by summation of force-field primitives. *J Neurosci* 20: 409–426, 2000b.

Kargo WJ, Rome LC. Functional morphology of proximal hindlimb muscles in the frog *Rana pipiens*. *J Exp Biol* 205: 1987–2004, 2002.

Krishnamoorthy V, Goodman S, Zatsiorsky V, Latash ML. Muscle synergies during shifts of the center of pressure by standing persons: identification of muscle modes. *Biol Cybern* 89: 152–161, 2003.

Krouchev N, Kalaska JF, Drew T. Sequential activation of muscle synergies during locomotion in the intact cat as revealed by cluster analysis and direct decomposition. *J Neurophysiol* 96: 1991–2010, 2006.

Lee DD, Seung HS. Learning the parts of objects by non-negative matrix factorization. *Nature* 401: 788–791, 1999.

Lee DD, Seung HS. Algorithms for non-negative matrix factorization. In: *Advances in Neural Information Processing Systems*, vol. 13, edited by Leen TK, Dietterich TG, Tresp V. Cambridge, MA: MIT, 2001, p. 556–562.

Li Q, Martin JH. Postnatal development of connectional specificity of corticospinal terminals in the cat. *J Comp Neurol* 447: 57–71, 2002.

Lockhart DB, Ting LH. Optimal sensorimotor transformations for balance. *Nat Neurosci* 10: 1329–1336, 2007.

Macpherson JM, Fung J. Weight support and balance during perturbed stance in the chronic spinal cat. *J Neurophysiol* 82: 3066–3081, 1999.

Magherini PC, Precht W, Richter A. Vestibulospinal effects on hindlimb motoneurons of the frog. *Pflügers Arch* 348: 211–223, 1974.

Mardia KV, Kent JT, Bibby JM. *Multivariate Analysis*. London: Academic, 1979.

McKay JL, Ting LH. Functional muscle synergies constrain force production during postural tasks. *J Biomech* 41: 299–306, 2008.

Miller LE. Limb movement: getting a handle on grasp. *Curr Biol* 14: 714–715, 2004.

Monaco V, Ghionzoli A, Micera S. Age-related modifications of muscle synergies and spinal cord activity during locomotion. *J Neurophysiol* 104: 2092–2102, 2010.

Mortin LI, Keifer J, Stein PS. Three forms of the scratch reflex in the spinal turtle: movement analyses. *J Neurophysiol* 53: 1501–1516, 1985.

Muceli S, Boye AT, d'Avella A, Farina D. Identifying representative synergy matrices for describing muscular activation patterns during multidirectional reaching in the horizontal plane. *J Neurophysiol* 103: 1532–1542, 2010.

Overduin SA, d'Avella A, Roh J, Bizzi E. Modulation of muscle synergy recruitment in primate grasping. *J Neurosci* 28: 880–892, 2008.

Perreault EJ, Chen K, Trumbower RD, Lewis G. Interactions with compliant loads alter stretch reflex gains but not intermuscular coordination. *J Neurophysiol* 99: 2101–2113, 2008.

Rathelot JA, Strick PL. Subdivisions of primary motor cortex based on cortico-motoneuronal cells. *Proc Natl Acad Sci USA* 106: 918–923, 2009.

Robertson GA, Mortin LI, Keifer J, Stein PS. Three forms of the scratch reflex in the spinal turtle: central generation of motor patterns. *J Neurophysiol* 53: 1517–1534, 1985.

Roh J. *Modules in the Brainstem and Spinal Cord Underlying Motor Behaviors* (PhD thesis). Cambridge, MA: Massachusetts Inst. of Technology, 2008.

Rubinson K. Projections of the optic tectum of the frog. *Brain Behav Evol* 1: 529–560, 1968.

Sabatini AM. Identification of neuromuscular synergies in natural upper-arm movements. *Biol Cybern* 86: 253–262, 2002.

Saltiel P, Tresch MC, Bizzi E. Spinal cord modular organization and rhythm generation: an NMDA iontophoretic study in the frog. *J Neurophysiol* 80: 2323–2339, 1998.

Saltiel P, Wyler-Duda K, d'Avella A, Tresch MC, Bizzi E. Muscle synergies encoded within the spinal cord: evidence from focal intraspinal NMDA iontophoresis in the frog. *J Neurophysiol* 85: 605–619, 2001.

Saltiel P, Wyler-Duda K, d'Avella A, Ajemian RJ, Bizzi E. Localization and connectivity in spinal interneuronal networks: the adduction-caudal extension-flexion rhythm in the frog. *J Neurophysiol* 94: 2120–2138, 2005.

Schepens B, Drew T. Independent and convergent signals from the pontomedullary reticular formation contribute to the control of posture and movement during reaching in the cat. *J Neurophysiol* 92: 2217–2238, 2004.

Shapovalov AI. Neuronal organization and synaptic mechanisms of supraspinal motorcontrol in vertebrates. *Rev Physiol Biochem Pharmacol* 72: 1–54, 1975.

Shinoda Y, Arnold AP, Asanuma H. Spinal branching of corticospinal axons in the cat. *Exp Brain Res* 26: 215–234, 1976.

Shinoda Y, Yokota J, Futami T. Divergent projection of individual corticospinal axons to motoneurons of multiple muscles in the monkey. *Neurosci Lett* 23: 7–12, 1981.

Shinoda Y, Yamaguchi T, Futami T. Multiple axon collaterals of single corticospinal axons in the cat spinal cord. *J Neurophysiol* 55: 425–448, 1986.

Stein PS, Victor JC, Field EC, Currie SN. Bilateral control of hindlimb scratching in the spinal turtle: contralateral circuitry contributes to the normal ipsilateral motor pattern of fictive rostral scratching. *J Neurosci* 15: 4343–4355, 1995.

Tantisira B, Alstermark B, Isa T, Kummel H, Pinter M. Motoneuronal projection pattern of single C3-C4 propriospinal neurons. *Can J Physiol Pharmacol* 74: 518–530, 1996.

Ting LH, Macpherson JM. A limited set of muscle synergies for force control during a postural task. *J Neurophysiol* 93: 609–613, 2005.

Torres-Oviedo G, Macpherson JM, Ting LH. Muscle synergy organization is robust across a variety of postural perturbations. *J Neurophysiol* 96: 1530–1546, 2006.

Torres-Oviedo G, Ting LH. Muscle synergies characterizing human postural responses. *J Neurophysiol* 98: 2144–2156, 2007.

Torres-Oviedo G, Ting LH. Subject-specific muscle synergies in human balance control are consistent across different biomechanical contexts. *J Neurophysiol* 103: 3084–3098, 2010.

Tresch MC, Cheung VC, d'Avella A. Matrix factorization algorithms for the identification of muscle synergies: evaluation on simulated and experimental data sets. *J Neurophysiol* 95: 2199–2212, 2006.

Tresch MC, Jarc A. The case for and against muscle synergies. *Curr Opin Neurobiol* 19: 1–7, 2009.

Tresch MC, Saltiel P, Bizzi E. The construction of movement by the spinal cord. *Nat Neurosci* 2: 162–167, 1999.

Tresch MC, Saltiel P, d'Avella A, Bizzi E. Coordination and localization in spinal motor systems. *Brain Res Brain Res Rev* 40: 66–79, 2002.

Weiss EJ, Flanders M. Muscular and postural synergies of the human hand. *J Neurophysiol* 92: 523–535, 2004.

Yakovenko S, Krouchev N, Drew T. Sequential activation of motor cortical neurons contributes to intralimb coordination during reaching in the cat by modulating muscle synergies. *J Neurophysiol* 105: 388–409, 2011.